Oxygen Adsorption on Spontaneously Reconstructed Au(511)

Fang Xu,[1] Matthew M. Montemore,[1,2] Christopher R. O'Connor,[1] Eri Muramoto,[2] Matthijs A. van Spronsen,[1] Robert J. Madix,[2] Cynthia M. Friend[1,2,*]

[1]Department of Chemistry and Chemical Biology, Harvard University, Cambridge, MA 02138, USA

[2]John A. Paulson School of Engineering and Applied Sciences, Harvard University, Cambridge, Massachusetts 02138, USA

Abstract:

The four-fold site on {100} facets, which are potential catalytic sites on high-curvature gold nanoparticles, is difficult to prepare on a gold single crystal due to surface reconstruction. Here, the Au(511) surface with a high density of step edges and a well-maintained {100} local structure was studied by scanning tunneling microscopy (STM), temperature programmed reaction spectroscopy (TPRS), and density functional theory (DFT) calculations. Annealing at 550 K and 870 K induces reconstruction on the Au(511) surface to a mixture of (311) and (711) micro-terraces. At room temperature and low oxygen coverage, oxygen adsorbs at both three- and four-fold sites on the surface, leading to a well-ordered zig-zag structure. Oxygen atoms cause significant orbital hybridization and a slight displacement of the gold atoms to which they bind. High oxygen coverages induce the formation of clusters, which are not active towards oxidation of isopropanol at room temperature and a pressure of 10^{-10} mbar. Oxygen adsorption saturates at 1 monolayer, and two separate oxygen recombinative desorption peaks were observed at coverages above 0.11 ML. Our characterization of this surface and the O adsorption structure allows future studies of {100} micro-terraces for oxidation reactions, which contributes to studies on gold-based catalysts with an irregular shape.

Keywords:

Gold surface; oxygen desorption; reconstruction; STM; DFT calculations

1. Introduction

An important overarching question in heterogeneous catalysis is whether the surface structure has a significant effect on reactivity. Gold-based catalysts catalyze oxidation processes, including CO oxidation and selective oxidation of alcohols, when adsorbed atomic oxygen is present [1, 2]. Some reactions have been reported to be structure sensitive. For example, gold nanorod catalysts with a higher percentage of Au(111) facets exhibit a higher selectivity towards the Sonogashira cross-coupling reaction between phenylacetylene and 4-iodoanisole than those with more (100) facets [3]. Further, dynamic surface structure-activity relationships are suggested by a study that combined environmental transmission electron microscopy and *ab initio* electronic calculations, indicating that CO actively adsorbs at on-top sites on half of the top layer of Au atoms on reconstructed {100} facets, whereas {111} facets are considered "oblivious" to CO [4]. Further, adsorption energies of O_2 and O, as well as interactions between adsorbed O atoms, have been shown to depend sensitively on the geometry of Au surfaces [5]. In principle,

structure sensitivity of bonding and reaction at the atomic level can be understood by using single-crystal models.

A significant challenge in studying extended gold surfaces with well-defined structures is the reconstruction that is typical during preparation in ultrahigh vacuum (UHV) conditions. The reconstructions tend to form denser packing of Au in the top layer, often yielding qualitatively similar local structures to the (111) surface. For instance, Au(111) reconstructs into the so-called herringbone structure with a compressed but still three-fold symmetric surface with a ($\sqrt{3}$×22) supercell [6]. Au(110) forms a (1×2) missing row structure to form (111) micro-facets locally [7]. Au(100) forms a commensurate c(28×48) structure so that two layers of quasi-hexagonal-packed layers overlap to form moiré patterns [8, 9]. In all of these cases, microfacets with three-fold coordination sites are predominant after reconstruction, rendering it challenging to study coordination sites with four-fold symmetry.

Unreconstructed surfaces may be present in sufficiently small nanoparticles [4, 10-12] because the reconstructions all occur over a long length scale. Specific to Au(100), the large-scale c(28×48) reconstruction eliminates the four-fold symmetric sites. Hence, to study these types of sites, our strategy is to investigate a single-crystal surface that retains (100) micro-terraces with the four-fold sites, i.e., Au(n11) surfaces (n = 3, 5, 7, 9, 11,…). Prior work using low energy electron diffraction (LEED) reported that Au(511) and Au(311) are stable upon annealing to 1073 K, while Au(711) and Au(911) reconstruct to a mixture of Au(100) and Au(511) structures [13]. Motivated by the prior study, Au(511) surface is studied herein because of the possibility of probing four-fold sites.

An un-reconstructed Au(511) surface would be composed of (100) micro-terraces spanning over 3 atomic rows (Fig. 1). Neighboring (100) micro-terraces are mismatched by a half atom along the [011] direction to form three-fold sites on the secondary step edges (Fig. 1A; a primary step edge is defined as the step edge of large-scale (511) terraces). The spacing between neighboring secondary step edges is 0.748 nm [14]. However, Ibach pointed out that LEED is not able to distinguish between a regular (511) surface and a mixture of (311) and (711) structures [15]. Thus, the structure of Au(511) surface remains uncertain.

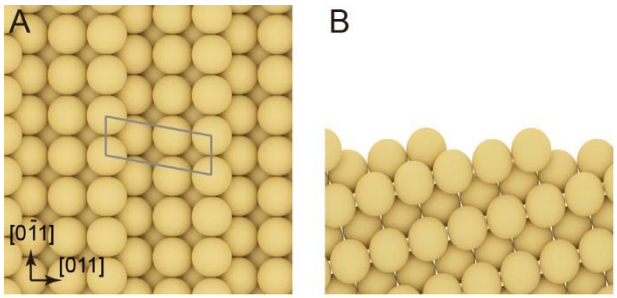

Figure 1. Idealized surface structure of Au(511) without reconstruction: (A) Top view and (B) side view of Au(511). A primitive unit cell is drawn in (A).

In this work, the temperature-dependent Au(511) reconstruction was identified by scanning tunneling microscopy (STM), showing that mixtures of (311) and (711) micro-terraces actually form on Au(511), in contrast to prior claims based on LEED [13]. The structure of oxygen pre-covered Au(511) surfaces was studied by STM, temperature programmed reaction spectroscopy (TPRS), and density functional theory (DFT). At low coverages, adsorbed oxygen forms a well-ordered zig-zag structure on the reconstructed Au(511) surface, occupying both three-fold and

four-fold sites. The adsorption induces some displacement of gold atoms bound to O and eventually causes the formation of clusters at high oxygen coverages. These clusters are less active than the lower-coverage structures for selective oxidation of isopropanol. The results contribute to the understanding of the local structure and the role of oxygen at gold-based catalysts with narrow terraces.

This paper is dedicated to the memory of our colleague and friend, Dr. Jan Hrbek—a tremendously creative and deep-thinking scientist, who was also a man of great courage. Jan escaped with his family from Czechoslovakia during a time of repression around 1980. He gave up a stable position to move to the US without any guarantee of employment. Through a series of fortunate events, he was offered a research position with Fritz Hoffman at EXXON Research, where he did extraordinary infrared studies on Ru [16]. Jan later moved to the Chemistry Department at Brookhaven National Laboratory (BNL) where he remained to the end of his research career. We were fortunate enough to have regular interactions with Jan at BNL because of our overlapping interest in the surface chemistry of Au and in the preparation of "inverse catalysts" [17, 18]. During his research career at BNL, Jan not only did superb work but also fostered the careers of his collaborators, many of whom are leading our field today. Jan also gave back to the broader community as a detailee serving as a program manager in the Catalysis Science program in the Chemical, Biological and Geological Sciences Division of Basic Energy Sciences in Department of Energy. With this issue, we all honor Dr. Jan Hrbek for his many contributions to surface chemistry and to the wider scientific community. He was exacting in his work and was extremely interested in understanding how surface structure affects chemical behavior; thus, we dedicate this article to Jan.

2. Methods

A Au(511) sample was cleaned by Ar^+ 15 min sputter - 20 min annealing cycles (Ar, Airgas east, ultra high purity grade). Surface oxygen atoms were prepared by thermal decomposition of ozone at room temperature using a direct dosing tube that was within 3 mm of the Au(511) surface. Ozone was produced using a commercialized ozone generator (ozone engineering, LG-7). The concentration of ozone was measured by a concentration monitor, Tele-dyne Instruments, Model 454H.

All STM experiments were conducted in a commercialized Omicron VT Beam Deflection AFM/STM chamber, which included an analysis chamber equipped with LEED and STM and a preparation chamber for sample treatment. The background pressure was 2×10^{-10} mbar. During experiments, LEED patterns were constantly checked to ensure no bulk reconstruction occurred. All STM measurements were conducted at room temperature with a Pt/Ir tip.

The sample used in STM measurements was later used for temperature programmed reaction spectroscopy (TPRS) experiments. Temperature programmed studies were conducted in a separate chamber with a background pressure $< 5 \times 10^{-10}$ Torr using a triple filter Hiden quadrupole mass spectrometer (QMS, HAL-Hiden/3F) and a heating rate of 1 K/s. The Au(511) crystal was further cleaned by several oxidation cycles using ozone and flash annealed to 700 K until no CO_2 desorbed from the surface. For TPRS experiments, the coverage of adsorbed oxygen was calibrated by the integrated area of O_2 desorption peak due to atomic oxygen recombination above 450 K. The saturation of the O_2 peak corresponds to 1 ML of atomic O on the surface.

Density functional theory (DFT) calculations were performed using the VASP code [19, 20] with the PBE functional [21] and Tkatchenko-Scheffler corrections [22]. The projector-augmented wave method was used for the core electrons [23, 24]. The calculated lattice constant for Au was 4.11 Å. For the Au(511) surface, a 4×1 surface cell was used with 12 layers (48 total Au atoms per unit cell). For the Au(311) surface, a 4×2 surface cell was used with 10 layers (80 Au atoms per unit cell). The k-point sampling grid was 7×7×1 for Au(511) and 5×5×1 for Au(311). STM image simulation was performed using the Tersoff-Hamann method [25]. Adsorption energies in this work were calculated as $E_{ad} = E_{slab} - E_{O,g} - E_{Au}$.

3. Results and Discussion

3.1 Structure of Au(511) surface

It is difficult to use LEED to determine the surface structure of Au(511) because of the complexity of the patterns, yet only LEED has been used to experimentally probe the Au(511) surface in UHV conditions [13]. The LEED pattern of many stepped metal surfaces containing (100) micro-terraces, such as Au(310),[26, 27] Cu(511) [28, 29], Cu(117) [30], Ag(115) [15], and Ni(771) [31], shows exactly the unreconstructed ideal surface. Unlike those surfaces, the LEED pattern of Au(511) surface contains extra spots along [011] direction, specifically reflecting 2.5 times the width of unreconstructed (100) micro-terraces (Fig. S1A). Additionally, the spot intensity changes with the beam energy (Fig. S1). Sotto and Boulliard ascribed the complexity of the pattern to contributions from both (511) and (100) facets, and long-range order over several micro-terraces [13]. However, as discussed before, other fcc {511} metal surfaces, which also contain (511) and (100) facets, do not show the extra spots. The as-prepared Au(511) must undergo reconstruction to some extent, which will be resolved by STM later in this work.

The Au(511) surface reconstructs to a mixture of bright double row and triple row units, observed in STM images (lines with double arrows in Fig. 2A, B). In each repeating unit, two or three bright rows separated by a wide dark row were imaged, with the former repeating unit being most prevalent. The total width of a double row unit is ~1.6 nm along the [011] direction and is comprised of bright double rows separated by ~0.5 nm and a dark row of ~1.1 nm, as measured in the line scan (Fig. 2C). The measured widths are similar to those predicted for terraces of regular (311) and (711) micro-terraces. Specifically, the width of a double row is similar to that of an idealized (311) terrace of 0.47 nm and the width of a triple row is similar to that of an idealized (711) terrace of 1.028 nm without top layer relaxation [14].

Based on the measured widths of the micro-terraces, a model was proposed for the double row unit (Fig. 2D). Peaks 1 and 2 in the line scan (Fig. 2C) correspond to the repeating secondary step edges of (711) and (311), respectively (Fig. 2D). The proposed double row structure, i.e. (311)-(711) repeating unit, fits well on a (511) substrate, as only one extra row of gold atoms (marked 1) is added or removed to every other regular (511) secondary step edge. We also note that the proposed model does not include surface relaxation, which is very likely to occur and can lead to small variations in the width.

An added row was often observed on the as-prepared Au(511) surface (Fig. 2A), which can be explained well by our proposed model. During the annealing process, extra gold atoms diffuse and form two rows on ascending secondary step edges of (711) micro-terrace (blue dashed boxes in Fig. 2D, 2E). As a result, neighboring (311) and (711) micro terraces switch position, that is, an added row causes a swap between a double row unit and a neighboring triple row unit, which agrees with the STM results.

A higher annealing temperature of 870 K induces the formation of more close-packed atoms in the top layer, evidenced by a higher density of triple row units and the increased roughness of the surface. The LEED pattern remains similar, despite an intensity change of a few spots (Fig. S2), which explains why previous LEED studies concluded that Au(511) was stable upon annealing at 1073 K [13]. The sample was cleaned for 60 sputter-annealing cycles such that no clusters were observed on the as-prepared surface using STM; thus, we believe the impurity level is negligible, i.e., the observed structural change in large scale was not induced by impurities.

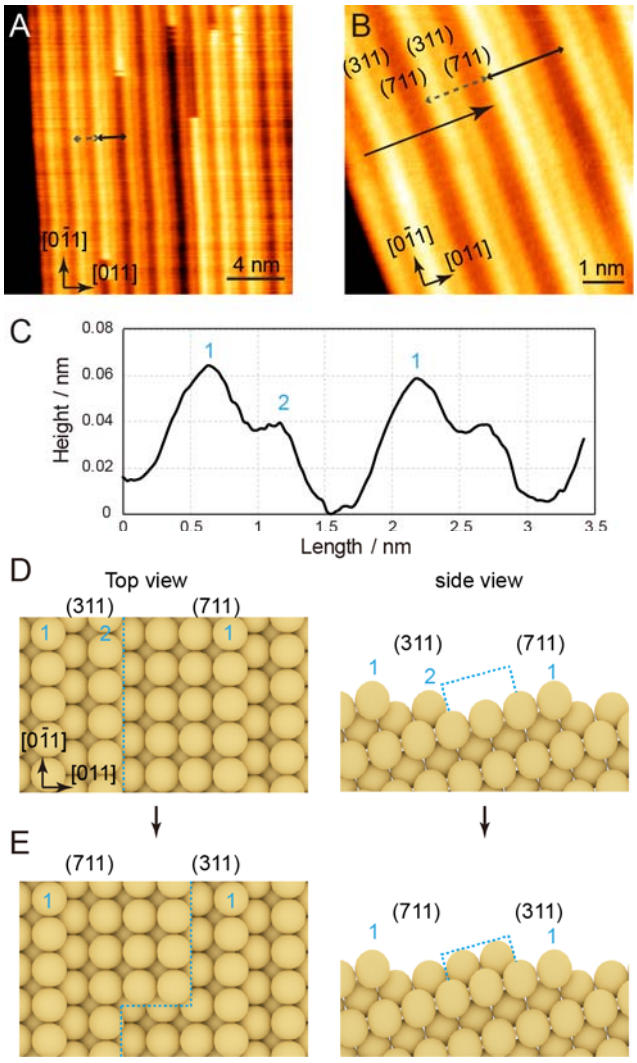

Figure 2. The Au(511) surface reconstructs to a mixture of (311) and (711) facets after cleaning and heating to 550 K, based on STM images. (A) and (B) show STM images of the terrace structure at two different magnifications. Grey and black dashed lines with double arrows indicate a double row unit and a triple row unit, respectively. (C) shows a line-scan from the image in (B). (D) depicts a proposed model without relaxation of the double row unit on the reconstructed Au(511) surface. The same gold rows 1 and 2 in (C) are also marked in (D). (E) Schematic of added rows. Scanning conditions for the images shown were 1.2 V; 0.20 – 0.35 nA.

Well-resolved STM images of the as-prepared Au(511) surface after annealing at 870 K indicate that terraces are covered with double- and triple-row units; the latter is dominant (Fig. 3A). The atoms in the row of the ascending secondary step edge can only be resolved with a

sharp tip (Fig. 3B). The repeating Au rows are marked as 1, 2, 3, and 4. According to the line scan of the atomically resolved image (Fig. 3C), the corrugations of the atoms marked 2, 3, and 4 are all ~0.02 nm; the spacing between neighboring atoms from 1 to 4 is ~0.5 nm; and the spacing between 4 and 1 is ~0.6 nm, which makes a total width of a triple row unit ~2.1 nm.

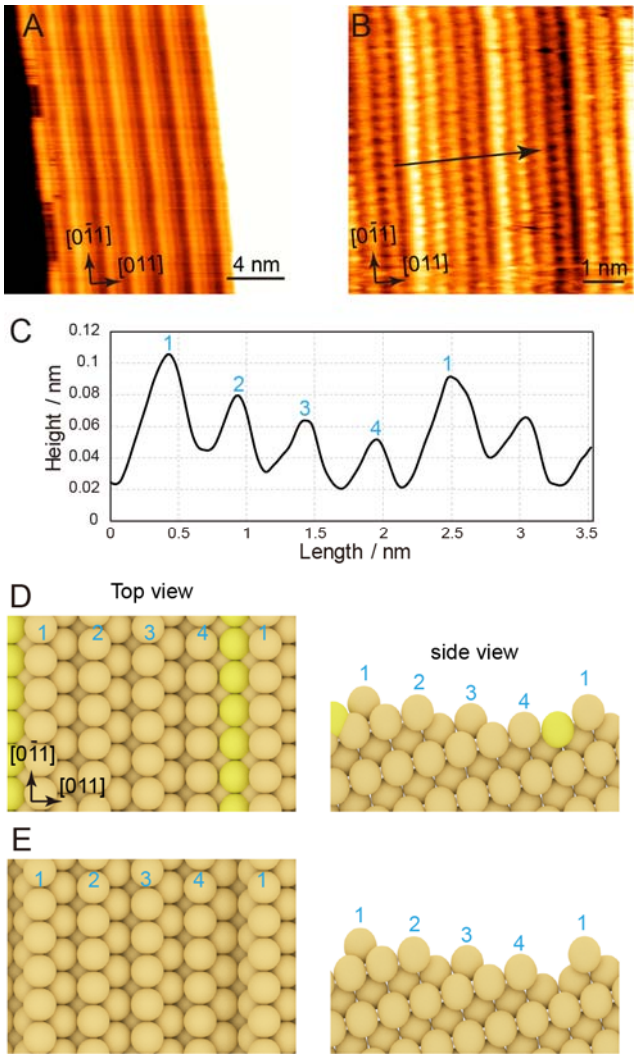

Figure 3. Reconstructed Au(511) surface after annealing at 870 K. (A) and (B) show the terrace structure. (B) shows the atomic structure of the triple rows. (C) The line-scan from (B). (D) and (E) Two proposed models of the triple row unit on as-prepared Au(511) without relaxation. A displaced row of gold atoms was highlighted as bright yellow in (D). Imaged gold rows on the surface were marked as 1, 2, 3, 4. Scanning conditions: 1.2 V; 0.20 – 0.35 nA.

Based on STM measurements, we propose two possible models of the triple row unit (Fig. 3D and 3E). The first model (Fig 3D) consists of (711)-(311)-(311) micro-terraces, where the second row next to the (711) secondary step edge (highlighted as bright yellow in Fig. 3D) moves slightly towards the bulk. Without the distortion of the highlighted gold, another atom is expected to be imaged between gold 4 and 1, which was not observed in Fig. 3C. This indicates that gold atoms in the top layers buckle due to some lattice mismatch and strain. The second model (Fig. 3E) consists of a missing row (711)-(311)-(311). In this model, the highlighted row of gold atoms is completely removed. Although the parameters agree well with the measured

values, the single row without neighbors (marked 1) is generally unstable by itself. Thus, we consider the first model as more likely.

A triple row unit contains one more (311) micro-terrace (more three-fold sites from the quasi-close-packed structure) than a double row unit. The extra (311) micro-terrace indicates the tendency to form a more close-packed structure at a higher annealing temperature, but results in an incommensurate top layer with the underlying (511) substrate. Extending the triple row unit results in a slight long-range incline of the surface (Fig. 3C). The fact that only relatively narrow primary terraces are observed (< 80 nm) indicates that the as-prepared Au(511) surface from 870 K is self-limited and is not able to form large-scale stable terraces.

After being annealed to 870 K, the Au(511) surface contains large areas of primary step bunches that form a different facet (Fig. 4). In some cases, the facet containing step bunches is even wider than the primary terrace. The Au(511) surface annealed at 550 K has fewer step bunches. The facet of step bunches is made of segments of rows and kinks, and is at an angle of 12.9° with respect to the (711)-(311)-(311) primary terrace. One possible facet that has kinks and this angle is the (46 6 -1) facet. The formation of kinks and increased roughness at elevated temperature were proposed by Dr. Schlößer on Ag(115) with energy parameters calculated.[32] Neighboring segments along the row direction are half row mismatched every time across a kink. The smallest spacing between parallel rows indicates the existence of the (311) micro terrace. Additionally, a unit cell is formed that has vectors of 4.35±0.1 nm (along rows) and 4.0±0.02 nm (across rows), angled ~70° between each other. The structure has more quasi-close-packed microstructures that are more thermodynamically stable than (100) microfacets in (511) and (711) terraces.

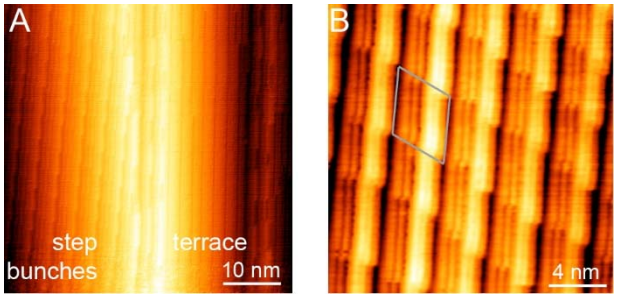

Figure 4. Step bunches on the reconstructed Au(511) surface. (A) The terrace structure and wide step bunches. (B) Zoomed in the structure of the step bunches with a unit cell drawn in a gray box. Scanning conditions: 1.4 – 1.5 V, 0.15 – 0.56 nA.

3.2 Oxygen Adsorption

At low oxygen coverages, adsorbed oxygen forms a well-ordered structure along secondary step edges, while at high coverages adsorbed oxygen forms amorphous clusters with the Au(511) substrate (Fig. 5). The oxygen adsorption structure is independent of the initial state of the Au(511) surface prepared at 550 K and 870 K (Fig. 5A and 5B). Oxygen atoms bound to the surface are imaged as dark features that alternate on each side of the Au ridges, i.e. alternating on three-fold and four-fold sites (an insert in Fig. 5A). At high oxygen coverages of ~0.5 ML, oxygen adsorption induces the formation of amorphous clusters (Fig. 5C). On the rough surface, the original gold rows are barely visible. The oxygen-induced roughness on as-prepared Au(511) is consistent with other gold surfaces [33, 34] and stepped metal surfaces, such as Cu(115) [29] and Cu(119) [35]. The clusters cannot be completely removed by flash annealing to 870 K, and

do not react with 9×10^{-10} mbar isopropanol at room temperature within 62 min. The remaining oxygen atoms were detected during post-annealing, confirming that O does not react (Fig. S3). As a comparison, isopropanol consumes well-ordered oxygen atoms rapidly on the Au(110) surface at room temperature [36]. The inertness of clusters agrees with previous work that high oxygen coverage has a negative effect towards catalytic reactions on gold surfaces [37, 38].

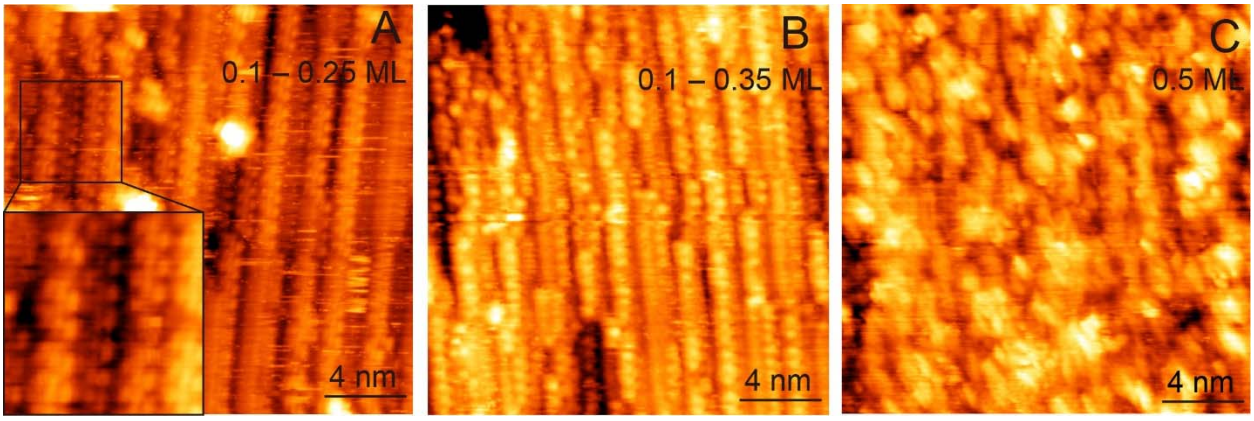

Figure 5. STM images of oxygen-covered, reconstructed Au(511) at room temperature. (A) Oxygen pre-covered surface that was previously annealed to 870 K (oxygen coverage of 0.1 – 0.25 ML). A zoomed in insert shows the adsorption structure. (B) Oxygen pre-covered surface that was previously annealed to 550 K (oxygen coverage at 0.1 – 0.35 ML). (C) surface with an oxygen coverage of ~0.5 ML. Scanning conditions: 1.36 – 1.5 V, 0.10 – 0.12 nA. Oxygen coverage was estimated by comparing the area of the oxygen recombination peak of the post-annealed surface in STM to standard peaks in Fig. 6.

Two distinct O_2 desorption features are observed for the recombination of O adsorbed on Au(511) (Fig. 6). The Au(511) surface was flash annealed at 700 K and 650 K separately, and no dependence on the initial state of the surface was observed, which agrees with STM results. At an oxygen coverage of 0.11 ML, only one desorption peak at 520 K (β_2) was observed. As the oxygen coverage increased to 0.35 ML, a second desorption peak emerged at 490 K (β_1). With increasing oxygen coverage, the low temperature peak (β_1) grew faster than the high temperature peak (β_2) until both peaks saturated at 1 ML. During the process, the β_2 peak shifted to a shoulder at 530 K, and the β_1 peak shifted to 520 K indicating an attractive interaction among corresponding surface oxygen atoms. For oxygen coverages < 0.50 ML, the β_2 desorption mechanism was responsible for the majority of O_2 desorption, while for oxygen coverages > 0.50 ML the β_1 desorption mechanism was dominant. The absence of new peaks as initial oxygen coverage increased indicates the microstructure of oxygen adsorption in clusters (Fig. 5C) and chains (Fig. 5A and 5B) are the same.

Base on a comparison between our results and the literature, the β_1 and β_2 peaks are very likely due to oxygen desorption from micro-terraces and secondary step edges, which correspond to four-fold and three-fold sites respectively, as shown with STM and DFT. Oxygen adsorption at high coverages shares a similar local structure with low coverages, as both peaks hold for all oxygen coverages investigated. The two oxygen recombinative desorption peaks were reported from other ozone-treated gold surfaces. On the Au(111) surface, one or two oxygen recombinative peaks appear at 520 – 600 K, depending on the oxygen coverage and heating rate [39, 40]. The two peaks are assigned as oxygen desorption from the “herringbone” reconstructed surface and the reconstruction-lifted surface due to high oxygen coverage (> 0.1 ML or > 40

Langmuir exposure). On the stepped gold surface Au(211) that contains (111) micro-terraces, two peaks at 540 K and 515 K are assigned to oxygen desorption from micro-terraces and secondary steps[41]. The peak at 530 K (micro-terraces) also shifts to a higher temperature as oxygen coverage increases, similarly to β_1 peak in this work. The stepped surface prohibits the formation of the "herringbone" reconstruction, thus, no additional peak was observed. On the Au(110)-(1×2) surface, the secondary desorption peak at a lower temperature (490 K), assigned as gold oxide, appears at coverages higher than 1.13 ML [42]. The other peak corresponds to monolayer adsorption. Interestingly, on the Au(100) surface, which spontaneously reconstructs under UHV conditions, no oxygen uptake was observed after being exposed to 600 L ozone [40]. However, if on Au(311) only one O_2 desorption peak around 550 K appears [40]. The peak was assigned as desorption from unreconstructed (111) sites. Apparently, the (100) micro-terraces on Au(311) surface were not maintained.

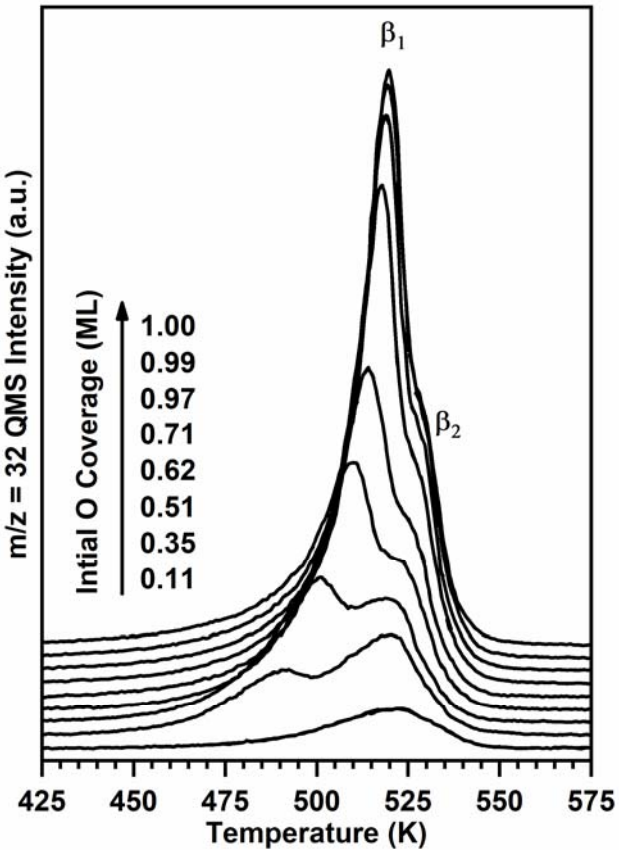

Figure 6. Two desorption features at 490 K (β_1) and 520 K (β_2) are observed for atomic oxygen recombination to O_2 on reconstructed Au(511). The coverage of the pre-covered oxygen varies between 0.11 to 1.00 ML, based on the integrated area of the recombinative O_2 peak (the saturation peak corresponds to 1 ML).

Line-shape analysis of recombinative oxygen desorption from O/Au(511) indicates complex desorption behavior. The high temperature peak (β_2) has no observable shift up to ≈ 0.5 ML, which indicates first order desorption kinetics. The kinetics for the β_2 peak at oxygen coverages > 0.5 ML cannot be determined because the peak position is indistinguishable as a small shoulder on the low temperature peak (β_1). The desorption of low temperature peak (β_1) shows an autocatalytic feature: (1) the steepness of the leading edge increases with coverage which

suggests an accelerated desorption process; (2) the peak position incrementally shifts toward higher temperature for all oxygen coverages. A similar autocatalytic desorption mechanism has been shown on O/Au(110); autocatalytic desorption of oxygen on Au(110) is attributed to the desorption of oxygen occurring from the perimeter of clusters or islands of oxygen atoms with an increase in reaction rate for smaller sizes [42, 43]. The complex desorption mechanism of recombinative oxygen desorption from Au(511) warrants further investigation.

3.4 DFT calculations

The binding of atomic oxygen on unreconstructed Au(311) and Au(511) surfaces was studied using DFT to model the structures present on the reconstructed surface described above (Figure 7, Table 1). The step edges of these surfaces have quite similar O adsorption properties. Because the local environment of steps on wider terraces, such as (711), is structurally identical to the steps on Au(511), we expect O adsorption on the steps of these wider terraces to behave quite similarly to the steps of Au(511). Therefore, we expect our Au(511) results to hold for the (711) micro terraces experimentally observed in the reconstruction.

At low coverage, O prefers the two-fold bridge site on both Au(311) and Au(511), with an identical adsorption energy of -3.53 eV (Fig. 7B, 7F). The three-fold hollow at the step is somewhat less favorable on Au(311) than Au(511) (Fig. 7A, 7E). (All step edges discussed in this section are secondary step edges.) The four-fold hollow at the upper step is even less favorable than the three-fold hollow, with an adsorption energy of -3.44 eV on Au(511) (isolated O in this site is not shown). O adsorption at this site is unstable on Au(311) and relaxes to the bridge site. On the (311) surface, two of the Au atoms in the four-fold site are at the bottom of a step, and therefore have higher coordination numbers than the corresponding atoms on Au(511). This higher coordination likely destabilizes the O atom in this site.

O becomes more stable upon formation of linear O-Au-O units, and these structures can form at Au step atoms [7]. A pair of O atoms forming this structure (Fig. 7C, 7G), are 0.04 and 0.13 eV more stable compared to isolated O in the bridge site, for Au(311) and Au(511) respectively. These values are comparable to 0.07 eV, previously calculated for Au(110) [7]. An O atom in a full zig-zag chain is even more stable, by 0.16 and 0.23 eV compared to an isolated O for Au(311) and Au(511) respectively (Fig. 7D, 7H). The difference between the energetics for (311) and (511) is likely due to the destabilization of the four-fold site, as half of the Au atoms that comprise this site have a different coordination number on the two micro-terraces.

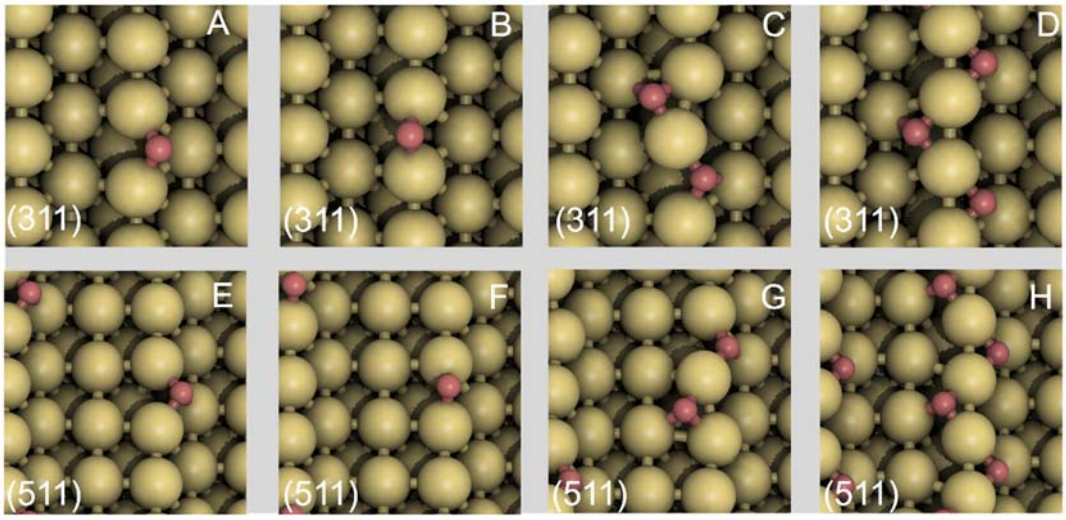

Figure 7. O adsorption geometries for O in the three-fold hollow (A, E), O in the bridge site (B, F), an O pair (C, G), and an O chain (D, H).

The O pair and O chain cause Au atoms to move vertically away from the bulk, similar to previous findings for Au(110) [7]. The Au step atoms in between an O pair move upward by approximately 0.06 to 0.07 nm, while the Au step atoms that are part of O-Au-O chains move vertically by roughly 0.06 nm. Additionally, the Au atoms shift to create a quasi-three-fold environment for the O atoms in the four-fold hollow (Fig. 7C, 7D, 7G, 7H). For the O-Au-O chain, this involves a horizontal translation of all of the step Au atoms by roughly 0.08 nm.

	Single O			
Surface	**three-fold hollow**	**bridge**	**O pair**	**O chain**
Au(311)	-3.43	-3.53	-3.57	-3.69
Au(511)	-3.45	-3.53	-3.66	-3.76
Au(211)		-3.55		
Au(110)	-3.68			

Table 1. Average O adsorption energies in eV for various O structures on stepped Au surfaces.

As part of previous work [44], we have calculated the adsorption energy of isolated O on the (1×2) missing-row reconstructed Au(110) surface and the Au(211) surface using comparable computational parameters. O adsorbs somewhat more strongly on Au(110) than on Au(511) and Au(311), by 0.13 eV. This is likely because the terrace atom of the three-fold site on Au(311) and Au(511) is more highly coordinated than on Au(110). On the Au(211) surface, isolated O adsorbs in the bridge site, which is very similar to the bridge site on Au(311) and Au(511). This is reflected in the similar adsorption energy on Au(211) of -3.55 eV [44].

Overall, the O adsorption trends across the (311), (511), (110), and (211) surfaces can be qualitatively understood by noting that (1) O atoms are more stable in sites with low-coordinated Au atoms, (2) O atoms prefer three-fold hollow sites, and (3) O atoms are stabilized by the formation of linear O-Au-O structural motifs. These three principles compete to determine site preference and binding strength at various sites, structures, and O coverages.

To gain further insight into the nature of the O-Au bond, we calculated the projected density of states (PDOS) for the bare Au(511) surface and for an O pair on Au(511) (Fig. 8). The results are similar to Au(110) [7]: Au atoms bound to an O atom hybridize significantly with O p states, which is particularly noticeable for the peaks at -6.7 eV and -0.7 eV. The Au atom with two O neighbors has significantly greater hybridization, while the Au with one neighbor is more similar to the bare Au case. In the energy range shown in Fig. 8, O p states and Au d states are the dominant contributions to the PDOS.

The O chain is the most stable O state on the surface, and thus we expect this state to be observed experimentally, except perhaps at very low O coverage. We therefore created simulated STM images for comparison with the experimental STM images (see Fig. 9). As expected, we observe a zig-zag shape along the Au ridge in the simulated STM images; a similar shape is observed in the experimental STM (Fig. 5). A similar O-chain structure has been observed in STM on Pd(119) [45], which is comparable to the (511) and (711) micro terraces.

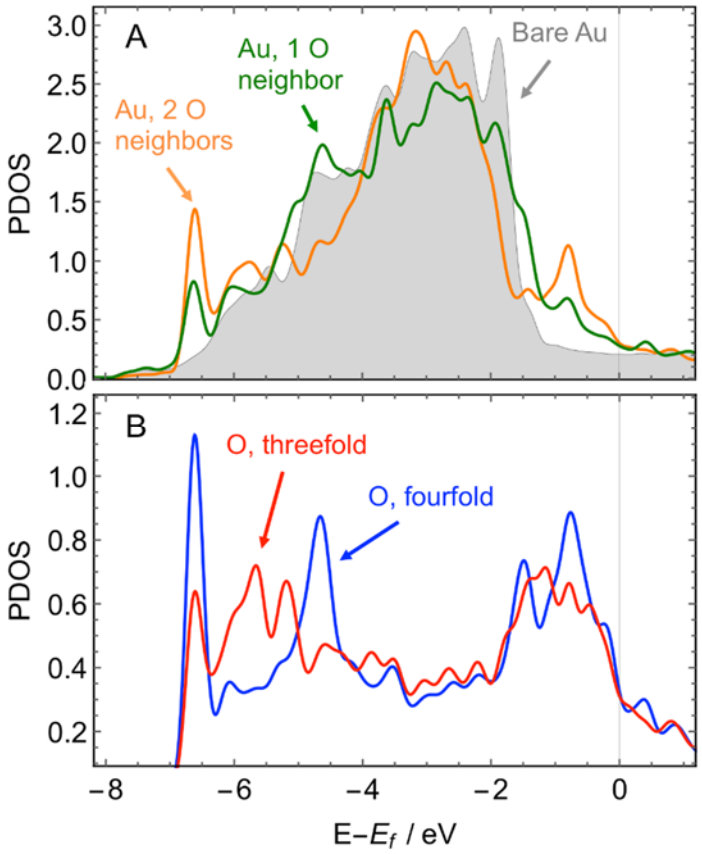

Figure 8. PDOS for two cases: bare Au(511) and an O pair on Au(511). In (A), the PDOS on step Au atoms is shown for both cases. In (B), the PDOS is shown on both O atoms in the O pair (see Figure 7G). Au step atoms are those that are less coordinated than Au(100) surface atoms.

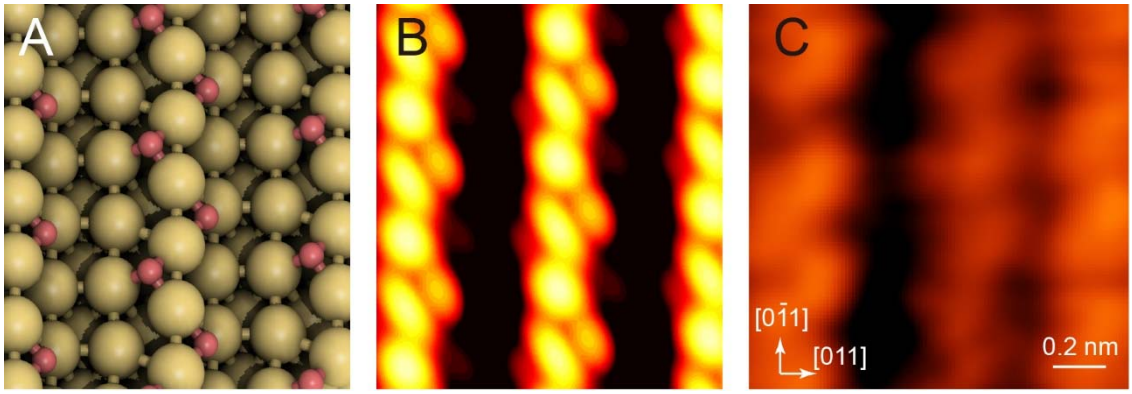

Figure 9. O chain structure on Au(511) (A), simulated STM of this structure (B), and a real STM image of the same scale (C).

4. Conclusion

The as-prepared Au(511) surface was studied by LEED and STM with two annealing temperatures of 550 K and 870 K. It was found that the surface is reconstructed to a mixture of (311) and (711) micro terraces along with step bunches. Furthermore, the surface reconstruction is temperature dependent: a higher annealing temperature leads to a higher density of (311) micro terraces that contain more close-packed local structures. Based on atomically resolved STM images, possible models were proposed for the dominant surface structure: a (311)-(711) double row unit was proposed for the low-temperature annealed surface, and a (311)-(311)-buckled (711) triple row unit was proposed for the high-temperature annealed surface. No evidence of a hexagonal-like reconstruction, as is seen on Au(100), was found.

The structure of oxygen adsorption on the as-prepared Au(511) surface was identified using STM and TPRS combined with DFT calculations. At low coverages, oxygen atoms form a well-ordered structure on the surface by exposure to ozone at room temperature. For isolated atoms, adsorption on the bridge site at the secondary step edge leads to the lowest adsorption energy on (100) micro terraces. For O pairs, adsorption on a gold atom at secondary step edges leads to a linear O-Au-O unit. Additionally, O pair adsorption on Au(311) was calculated to be 0.09 eV less stable than on Au(511) secondary step edges, which is ascribed to a different coordination number of the binding gold atoms. Zig-zag O chains form in an alternating structure on Au secondary step edges, occupying both four-fold and three-fold sites, which agrees with the observation of two oxygen recombinative peak at oxygen coverage above 0.11 ML from TPRS. In other cases where O chain formation is found, the ends of the O chains are generally more reactive towards oxidation of other species (e.g., CO or CO_2) [7, 46], and we expect this to be true for Au(511) as well. Trends in the O binding strength can be qualitatively understood based on the coordination number of the O, the coordination number of the Au atoms that the O is bound to, and the stabilization from O-O interactions across steps. At high coverages, the surface is severely roughened by the formation of clusters, which are less active than oxygen chains towards O-H bond cleavage of isopropanol.

The results contribute to fundamental understanding of highly stepped sites and high curvature sites of nanoparticle-based catalysts for oxidation reactions at various temperatures, since the local environment on the catalysts can be similar to those discussed in this work.

Highly stepped surfaces with micro terraces are also an ideal model system when long-range ordered surface terminations are not stable or easily reconstruct.

Corresponding Author

The corresponding author of this work is Prof. Cynthia M. Friend, who can be reached by friend@fas.harvard.edu.

Supporting Information

Supporting information includes additional STM and LEED results, as well as lattice vectors and relaxed Cartesian coordinates of the structures from density functional theory calculations.

Acknowledgment

This work was financially supported as part of the Integrated Mesoscale Architectures for Sustainable Catalysis (IMASC), an Energy Frontier Research Center (EFRC) funded by the US Department of Energy (DOE), Office of Science, Basic Energy Sciences under award no. DE-SC0012573.

Reference

[1] M.L. Personick, B. Zugic, M.M. Biener, J. Biener, R.J. Madix, C.M. Friend, Ozone-Activated Nanoporous Gold: A Stable and Storable Material for Catalytic Oxidation, ACS Catal., 5 (2015) 4237-4241.
[2] B. Zugic, L. Wang, C. Heine, D.N. Zakharov, B.A.J. Lechner, E.A. Stach, J. Biener, M. Salmeron, R.J. Madix, C.M. Friend, Dynamic restructuring drives catalytic activity on nanoporous gold–silver alloy catalysts, Nature Materials, 16 (2016) 558-564.
[3] J. Lin, H. Abroshan, C. Liu, M. Zhu, G. Li, M. Haruta, Sonogashira cross-coupling on the Au(111) and Au(100) facets of gold nanorod catalysts: Experimental and computational investigation, J. Catal., 330 (2015) 354-361.
[4] H. Yoshida, Y. Kuwauchi, J.R. Jinschek, K. Sun, S. Tanaka, M. Kohyama, S. Shimada, M. Haruta, S. Takeda, Visualizing Gas Molecules Interacting with Supported Nanoparticulate Catalysts at Reaction Conditions, Science, 335 (2012) 317-319.
[5] M.M. Montemore, M.A. van Spronsen, R.J. Madix, C.M. Friend, O2 Activation by Metal Surfaces: Implications for Bonding and Reactivity on Heterogeneous Catalysts, Chemical Reviews, 118 (2018) 2816-2862.
[6] S. Narasimhan, D. Vanderbilt, Elastic stress domains and the herringbone reconstruction on Au(111), Phys. Rev. Lett., 69 (1992) 1564-1567.
[7] F. Hiebel, M.M. Montemore, E. Kaxiras, C.M. Friend, Direct visualization of quasi-ordered oxygen chain structures on Au(110)-(1×2), Surf. Sci., 650 (2016) 5-10.
[8] R. Hammer, A. Sander, S. Förster, M. Kiel, K. Meinel, W. Widdra, Surface reconstruction of Au(001): High-resolution real-space and reciprocal-space inspection, Physical Review B, 90 (2014) 035446.
[9] O.K. Binnig, H. Rohrer, C. Gerber, E. Stoll, Real-space observation of the reconstruction of Au(100), Surf. Sci., 144 (1984) 321-335.
[10] T. Fujita, P. Guan, K. McKenna, X. Lang, A. Hirata, L. Zhang, T. Tokunaga, S. Arai, Y. Yamamoto, N. Tanaka, Y. Ishikawa, N. Asao, Y. Yamamoto, J. Erlebacher, M. Chen, Atomic origins of the high catalytic activity of nanoporous gold, Nat Mater, 11 (2012) 775-780.
[11] Z.L. Wang, Transmission Electron Microscopy of Shape-Controlled Nanocrystals and Their Assemblies, The Journal of Physical Chemistry B, 104 (2000) 1153-1175.

[12] T. Akita, M. Okumura, K. Tanaka, M. Kohyama, M. Haruta, TEM observation of gold nanoparticles deposited on cerium oxide, Journal of Materials Science, 40 (2005) 3101-3106.
[13] M. Sotto, J.C. Boulliard, Thermally induced transitions on clean stepped gold surfaces through LEED, Surf. Sci., 214 (1989) 97-110.
[14] I.-K. Suh, H. Ohta, Y. Waseda, High-temperature thermal expansion of six metallic elements measured by dilatation method and X-ray diffraction, Journal of Materials Science, 23 (1988) 757-760.
[15] H. Ibach, Electron energy loss spectroscopy of the vibration modes of water on Ag(100) and Ag(115) surfaces and comparison to Au(100), Au(111) and Au(115), Surface Science, 606 (2012) 1534-1541.
[16] I.J. Malik, J. Hrbek, RU3(CO)12 AND MO(CO)6 ADSORBED ON RU(001) AND AU/RU - AN INFRARED REFLECTION-ABSORPTION STUDY, Journal of Electron Spectroscopy and Related Phenomena, 54 (1990) 479-488.
[17] Z. Song, T.H. Cai, J.A. Rodriguez, J. Hrbek, A.S.Y. Chan, C.M. Friend, A novel growth mode of Mo on Au (111) from a Mo(CO)(6) precursor: An STM study, J. Phys. Chem. B, 107 (2003) 1036-1043.
[18] J.A. Rodriguez, P. Liu, J. Graciani, S.D. Senanayake, D.C. Grinter, D. Stacchiola, J. Hrbek, J. Fernández-Sanz, Inverse Oxide/Metal Catalysts in Fundamental Studies and Practical Applications: A Perspective of Recent Developments, The Journal of Physical Chemistry Letters, (2016) 2627-2639.
[19] G. Kresse, J. Furthmüller, Efficiency of ab-initio total energy calculations for metals and semiconductors using a plane-wave basis set, Computational Materials Science, 6 (1996) 15-50.
[20] G. Kresse, J. Hafner, Ab initio molecular dynamics for liquid metals, Physical Review B, 47 (1993) 558-561.
[21] J.P. Perdew, K. Burke, M. Ernzerhof, Generalized Gradient Approximation Made Simple, Phys. Rev. Lett., 77 (1996) 3865-3868.
[22] A. Tkatchenko, M. Scheffler, Accurate Molecular Van Der Waals Interactions from Ground-State Electron Density and Free-Atom Reference Data, Phys. Rev. Lett., 102 (2009) 073005.
[23] G. Kresse, D. Joubert, From ultrasoft pseudopotentials to the projector augmented-wave method, Physical Review B, 59 (1999) 1758-1775.
[24] P.E. Blöchl, Projector augmented-wave method, Physical Review B, 50 (1994) 17953-17979.
[25] J. Tersoff, D.R. Hamann, Theory of the scanning tunneling microscope, Physical Review B, 31 (1985) 805-813.
[26] M.A. van Spronsen, K.-J. Weststrate, A. den Dunnen, M.E. van Reijzen, C. Hahn, L.B.F. Juurlink, Hydrophilic Interaction Between Low-Coordinated Au and Water: H2O/Au(310) Studied with TPD and XPS, The Journal of Physical Chemistry C, 120 (2016) 8693-8703.
[27] M.E. van Reijzen, M.A. van Spronsen, J.C. Docter, L.B.F. Juurlink, CO and H2O adsorption and reaction on Au(310), Surf. Sci., 605 (2011) 1726-1731.
[28] J. Braun, J.P. Toennies, G. Witte, A SPALEED structural study of cesium adsorption on stepped copper surfaces Cu(211) and Cu(511), Surf. Sci., 340 (1995) 265-280.
[29] A.N. Chaika, S.S. Nazin, S.I. Bozhko, Selective STM imaging of oxygen-induced Cu(115) surface reconstructions with tungsten probes, Surf. Sci., 602 (2008) 2078-2088.
[30] S. Walter, H. Baier, M. Weinelt, K. Heinz, T. Fauster, Quantitative determination of Cu(117) multilayer surface relaxations by LEED, Physical Review B, 63 (2001) 155407.

[31] O. Haase, R. Koch, M. Borbonus, K.H. Rieder, Role of regular steps on the formation of missing-row reconstructions: Oxygen chemisorption on Ni(771), Phys. Rev. Lett., 66 (1991) 1725-1728.
[32] M.S. Hoogeman, D.C. Schlößer, J.B. Sanders, L. Kuipers, J.W.M. Frenken, Surface energetics and thermal roughening of Ag(115) studied with STM movies, Physical Review B, 53 (1996) R13299-R13302.
[33] F. Hiebel, S. Karakalos, Y. Xu, C.M. Friend, R.J. Madix, Structural Differentiation of the Reactivity of Alcohols with Active Oxygen on Au(110), Top. Catal., 61 (2017) 299-307.
[34] R.G. Quiller, T.A. Baker, X. Deng, M.E. Colling, B.K. Min, C.M. Friend, Transient hydroxyl formation from water on oxygen-covered Au(111), The Journal of Chemical Physics, 129 (2008) 064702.
[35] N. Reinecke, E. Taglauer, The kinetics of oxygen-induced faceting of Cu(115) and Cu(119) surfaces, Surf. Sci., 454-456 (2000) 94-100.
[36] F. Xu, R. Madix, C. Friend, Spatially Nonuniform Reaction Rates during Selective Oxidation on Gold, submitted.
[37] B. Xu, X. Liu, J. Haubrich, R.J. Madix, C.M. Friend, Selectivity Control in Gold-Mediated Esterification of Methanol, Angewandte Chemie International Edition, 48 (2009) 4206-4209.
[38] J. Gong, C.B. Mullins, Surface Science Investigations of Oxidative Chemistry on Gold, Accounts of Chemical Research, 42 (2009) 1063-1073.
[39] N. Saliba, D.H. Parker, B.E. Koel, Adsorption of oxygen on Au(111) by exposure to ozone, Surf. Sci., 410 (1998) 270-282.
[40] I. Nakamura, A. Takahashi, T. Fujitani, Selective Dissociation of O3 and Adsorption of CO on Various Au Single Crystal Surfaces, Catalysis Letters, 129 (2009) 400-403.
[41] J. Kim, E. Samano, B.E. Koel, Oxygen adsorption and oxidation reactions on Au(211) surfaces: Exposures using O2 at high pressures and ozone (O3) in UHV, Surf. Sci., 600 (2006) 4622-4632.
[42] J.M. Gottfried, K.J. Schmidt, S.L.M. Schroeder, K. Christmann, Oxygen chemisorption on Au(110)-(1×2) I. Thermal desorption measurements, Surf. Sci., 525 (2003) 184-196.
[43] J.M. Gottfried, K.J. Schmidt, S.L.M. Schroeder, K. Christmann, Oxygen chemisorption on Au(1 1 0)-(1×2) II. Spectroscopic and reactive thermal desorption measurements, Surf. Sci., 525 (2003) 197-206.
[44] M.M. Montemore, R.J. Madix, E. Kaxiras, How Does Nanoporous Gold Dissociate Molecular Oxygen?, The Journal of Physical Chemistry C, 120 (2016) 16636-16640.
[45] F. Li, F. Allegretti, S. Surnev, F.P. Netzer, Y. Zhang, W.B. Zhang, K. Reuter, Oxygen adsorption on stepped Pd(100) surfaces, Surf. Sci., 604 (2010) 1813-1819.
[46] I. Stensgaard, E. Laegsgaard, F. Besenbacher, The reaction of carbon dioxide with an oxygen precovered Ag(110) surface, The Journal of Chemical Physics, 103 (1995) 9825-9831.